

Complex-temperature properties of the Ising model on 2D heteropolygona lattices

Victor Matveev[†] and Robert Shrock[‡]

Institute for Theoretical Physics, State University of New York, Stony Brook, NY 11794-3840,
USA

Received 7 March 1995, in final form 6 June 1995

Abstract. Using exact results, we determine the complex-temperature phase diagrams of the 2D Ising model on three regular heteropolygona lattices, $(3 \cdot 6 \cdot 3 \cdot 6)$ (kagomé), $(3 \cdot 12^2)$ and $(4 \cdot 8^2)$ (bathroom tile), where the notation denotes the regular n -sided polygons adjacent to each vertex. We also work out the exact complex-temperature singularities of the spontaneous magnetization. A comparison with the properties on the square, triangular, and hexagonal lattices is given. In particular, we find the first case where, even for isotropic spin–spin exchange couplings, the non-trivial non-analyticities of the free energy of the Ising model lie in a two-dimensional, rather than one-dimensional, algebraic variety in the $z = e^{-2K}$ plane.

1. Introduction

The Ising model has long served as a prototype of a statistical mechanical system which undergoes a phase transition with associated spontaneous symmetry breaking and long-range order. The Ising model on a dimension $d = 2$ lattice has the great appeal that (for the spin- $\frac{1}{2}$ case with nearest-neighbour interactions) it is exactly solvable; for the square lattice, in the absence of an external magnetic field H , the free energy was first calculated by Onsager [1], and a closed-form expression for the spontaneous magnetization was first derived by Yang [2]. Later, the zero-field model was also solved for the triangular and hexagonal (= honeycomb) lattices; for a comparative review of the solutions on these three lattices, see [3]. However, in addition to the square, triangular, and hexagonal lattices, which involve tilings of the plane by one type of regular polygon, there are also other 2D lattices which have the property that all vertices are equivalent and all bonds (links) are of equal length, but are comprised of tilings by more than one type of regular polygons. We shall denote the regular 2D lattices which are comprised of tilings by one type of polygon as ‘homopolygona l’ and those involving tilings by more than one type of polygon as ‘heteropolygona l’. Indeed, as will be discussed further below, the (zero-field) free energy and spontaneous magnetization for the Ising model have been calculated for three heteropolygona l 2D lattices. The results yield valuable insights into how the properties of the solution depend on the tiling of the plane and, in particular, how they change when this tiling involves more than one kind of polygon.

In this paper, we shall determine the complex-temperature phase diagrams and singularities of the spontaneous magnetization for the three particular heteropolygona l

[†] E-mail address: vmatveev@max.physics.sunysb.edu

[‡] E-mail address: shrock@max.physics.sunysb.edu

lattices for which the Ising model has been solved. There are several reasons for studying the properties of statistical mechanical systems such as spin models with the temperature variable generalized to take on complex values. First, one can understand more deeply the behaviour of various thermodynamic quantities by seeing how they behave as analytic functions of complex temperature. Second, one can see how the physical phases of a given model generalize to regions in appropriate complex-temperature variables. Third, a knowledge of the complex-temperature singularities of quantities which have not been calculated exactly helps in the search for exact closed-form expressions for these quantities. This applies, in particular, to the susceptibility of the 2D Ising model. Complex-temperature properties of the Ising model (zeros of the partition function and singularities of thermodynamic and response functions) have been explored in a number of papers for homopolygona 2D lattices and for various 3D lattices [4–13]. ([8] and part of [5, 6] deal with the $d = 3$ Ising model.) However, to our knowledge, analogous investigations of complex-temperature properties have not been reported for heteropolygona 2D lattices.

To begin, we need to describe the heteropolygona lattices. We shall use the standard mathematical notation for general lattices [14]. A regular tiling of the plane is defined as one involving one or more regular polygons, i.e. polygons each of whose sides are of equal length. An Archimedean lattice is defined as a regular tiling of the plane in which all vertices are equivalent. Thus each vertex has the same coordination number, which we shall denote as q . From the definition, it follows immediately that all of the bonds on an Archimedean lattice are of equal length. For this reason, it is natural to consider the case of equal spin–spin couplings, and we shall do this here. However, it should be noted that the bonds on an Archimedean lattice are not, in general, all equivalent. For the three homopolygona Archimedean lattices, it is obvious that all bonds are equivalent, but for the heteropolygona lattices, this equivalence only holds if (i) the lattice consists of only two types of polygons and (ii) each edge of the first type of polygon is also an edge of the second type of polygon. Among the eight heteropolygona Archimedean lattices, this condition is met only for the $(3 \cdot 6 \cdot 3 \cdot 6)$ (kagomé) lattice (see below). The mathematical definition of, and notation for, an Archimedean lattice Λ are specified by $\Lambda = (\prod_{j=1}^q p_j)$, where p denotes a regular p -gon. The meaning of this symbol is that as one makes a small circuit around any vertex, one traverses first the polygon p_1 , next p_2 , and so forth, finally traversing p_q . If a p -sided polygon occurs ℓ times sequentially in this product, one signifies this by p^ℓ . There are 11 such ($d = 2$) Archimedean lattices [14]. Of the 11 Archimedean lattices, three are homopolygona. These are the well known square, triangular, and hexagonal lattices, which are denoted, respectively, (4^4) , (3^6) , and (6^3) . Note that the dual of a homopolygona lattice (p^ℓ) is (ℓ^p) , so that it is self-dual if and only if $p = \ell$, which occurs only for $p = 4$. The other eight Archimedean lattices are heteropolygona. These lattices are listed in table 1. (One lattice, $(3^4 \cdot 6)$, occurs in two enantiomorphic (chiral) forms, which are considered together here.)

The three heteropolygona Archimedean lattices for which we shall determine the complex-temperature phase diagrams and singularities of the magnetization are those for which the Ising model has been solved exactly, namely the (i) $(3 \cdot 6 \cdot 3 \cdot 6)$, (ii) $(3 \cdot 12^2)$ and (iii) $(4 \cdot 8^2)$ lattices. For the reader's convenience, these lattices are shown in figures 1–3, respectively. The $(3 \cdot 6 \cdot 3 \cdot 6)$ and $(4 \cdot 8^2)$ lattices are often denoted kagomé and bathroom tile, respectively. In the literature, the $(3 \cdot 12^2)$ and $(4 \cdot 8^2)$ lattices are frequently denoted by the shorthand symbols 3–12 and 4–8. As was observed by Utiyama [15], one way to construct these lattices is to start from a checkerboard lattice, replace each 'black' square by a square with n_v additional vertical bonds, and then take certain of the spin–spin couplings either to 0 or ∞ . One chooses $n_v = 1$ to construct the $(3 \cdot 6 \cdot 3 \cdot 6)$ and $(4 \cdot 8^2)$ lattices, and $n_v = 3$

Table 1. Table of the 11 Archimedean lattices. The first three are the well known homopolygonal lattices, and the remaining eight are heteropolygonal. The entries in the column denoted Bip. indicate whether (Y, N) the lattice is bipartite. The entries in the column denoted ‘Sym.’ indicate whether the complex-temperature phase diagram and zeros of the partition function for the (spin- $\frac{1}{2}$, zero-field) Ising model have the symmetries $z \rightarrow -z$ and/or $z \rightarrow 1/z$, or neither, denoted by ‘n’.

Lattice	Name	q	Bip.	Sym.
(3^6)	Triangular	6	N	$z \rightarrow -z$
(4^4)	Square	4	Y	$z \rightarrow -z, z \rightarrow 1/z$
(6^3)	Hexagonal	3	Y	$z \rightarrow 1/z$
$(3 \cdot 6 \cdot 3 \cdot 6)$	Kagomé	4	N	$z \rightarrow -z$
$(3 \cdot 12^2)$	—	3	N	n
$(4 \cdot 8^2)$	Bathroom tile	3	Y	$z \rightarrow 1/z$
$(3^4 \cdot 6)$	—	5	N	n
$(3^3 \cdot 4^2)$	—	5	N	n
$(3^2 \cdot 4 \cdot 3 \cdot 4)$	—	5	N	n
$(3 \cdot 4 \cdot 6 \cdot 4)$	—	4	N	$z \rightarrow -z$
$(4 \cdot 6 \cdot 12)$	—	3	Y	$z \rightarrow 1/z$

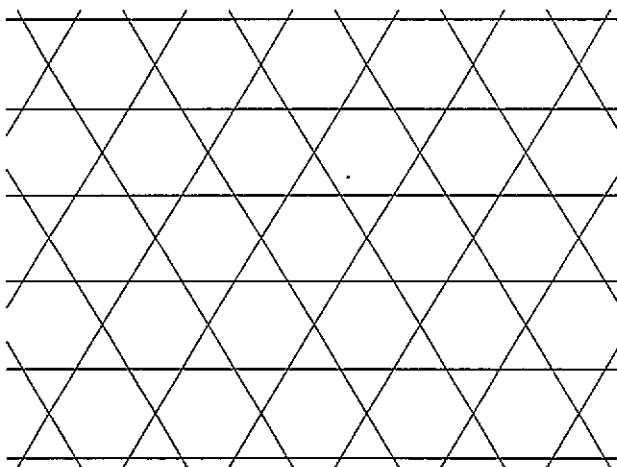
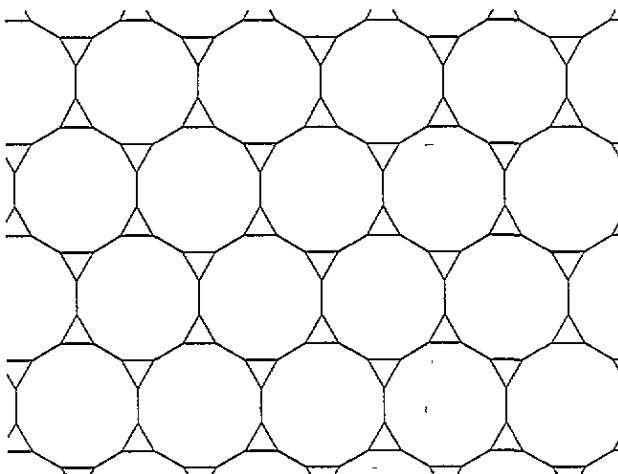
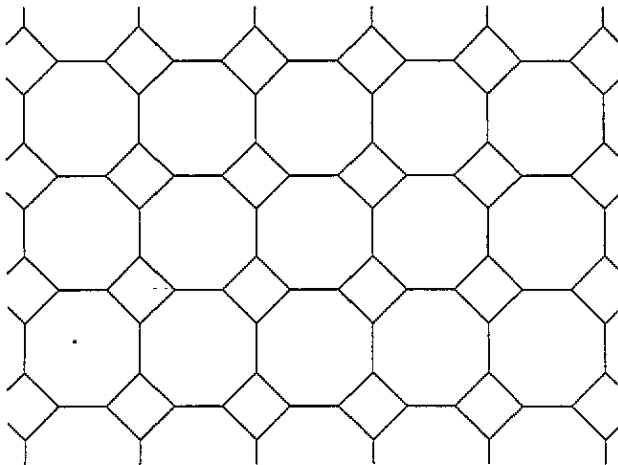


Figure 1. The $(3 \cdot 6 \cdot 3 \cdot 6)$ (kagomé) lattice.

to construct the $(3 \cdot 12^2)$ lattice. Using this observation, Utiyama discussed ingredients for an exact solution for the (zero-field) free energy for these lattices [15]. These lattices can also be obtained by (possibly iterated) decoration and/or star-triangle operations from the three homopolygonal lattices [16].

We recall that abstractly, the duality mapping for a d -dimensional lattice maps k -cells to $d - k$ cells. In our present case, with $d = 2$, this mapping interchanges 0-cells (vertices) and 2-cells (polygonal faces) while taking 1-cells (bonds) to other bonds. The duals of Archimedean lattices are Archimedean if and only if they are homopolygonal; for the heteropolygonal Archimedean lattices, the dual lattices are of a different type, called Laves lattices in the mathematical literature [14, 17]. A Laves lattice is defined as a regular tiling of the plane involving a single (in general, non-regular) polygon. Thus, the bonds of a Laves lattice are not, in general, of equal length, and the vertices (sites) are not, in general, equivalent. There is a one-to-one correspondence, namely that of duality, between the 11 Archimedean lattices and the 11 Laves lattices. Clearly, the number of different types of

Figure 2. The $(3 \cdot 12^2)$ lattice.Figure 3. The $(4 \cdot 8^2)$ (bathroom tile) lattice.

0-cells (vertices) on the Laves lattice Λ^* which is the dual of the Archimedean lattice Λ is equal to the number of different 2-cells (polygons) on Λ . Similarly, the fact that the Laves lattice consists of only one type of (generally non-regular) 2-cell (polygon) follows, by duality, from the fact that its dual Archimedean lattice consists of only one type of 0-cell (vertex). For example, the Laves lattice $[4 \cdot 8^2]$, commonly called the Union Jack lattice, which is dual to the $(4 \cdot 8^2)$ (bathroom tile) lattice, is shown in figure 4.

The solution for the (zero-field) free energy on each of the Archimedean lattices immediately gives the solution on the corresponding dual Laves lattice. Thus, our determination of the complex-temperature phase diagrams for the three heteropolygonal Archimedean lattices considered here also yields a corresponding determination of the complex-temperature phase diagrams for their dual Laves lattices.

2. Model and notation

Our notation is standard, so we review it here only briefly. We consider the spin- $\frac{1}{2}$ Ising model on the 2D lattices Λ as discussed above at a temperature T and external magnetic

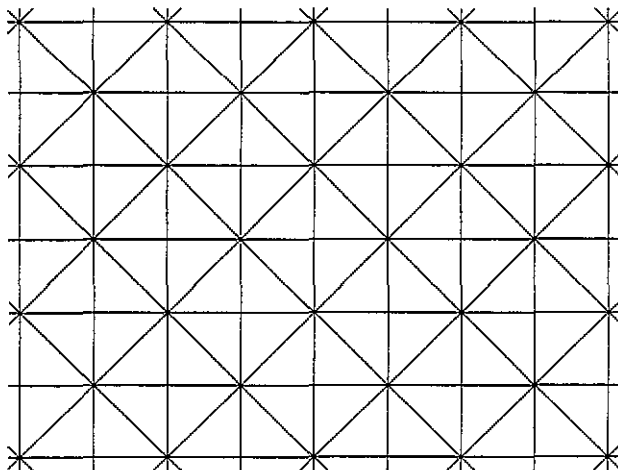


Figure 4. The $[4 \cdot 8^2]$ (Union Jack) lattice, which is the Laves lattice dual to the Archimedean lattice $(4 \cdot 8^2)$.

field H (where $H = 0$ unless otherwise specified) defined by the partition function

$$Z = \sum_{\{\sigma_n\}} e^{-\beta \mathcal{H}} \quad (2.1)$$

with the Hamiltonian

$$\mathcal{H} = -J \sum_{\langle nn' \rangle} \sigma_n \sigma_{n'} - H \sum_n \sigma_n \quad (2.2)$$

where $\sigma_n = \pm 1$ are the Z_2 spin variables on each site n of the lattice Λ , $\beta = (k_B T)^{-1}$, J is the exchange constant, $\langle nn' \rangle$ denote nearest-neighbour sites, and the units are defined such that the magnetic moment which would multiply the $H \sum_n \sigma_n$ is unity. (Hereafter, we shall use the term 'Ising model' to denote the spin model unless otherwise indicated.) We use the usual notation $K = \beta J$, $h = \beta H$, $v = \tanh K$, $z = e^{-2K}$, $u = z^2 = e^{-4K}$, and $\mu = e^{-2h}$. Note that v and z are related by the bilinear conformal transformation

$$z = \frac{1-v}{1+v}. \quad (2.3)$$

We record the symmetries

$$K \rightarrow -K \Rightarrow \{v \rightarrow -v, z \rightarrow 1/z, u \rightarrow 1/u\}. \quad (2.4)$$

It will also be useful to introduce the common abbreviations

$$C \equiv \cosh(2K) \quad (2.5)$$

$$S \equiv \sinh(2K). \quad (2.6)$$

The reduced free energy per site is $f = -\beta F = \lim_{N_s \rightarrow \infty} N_s^{-1} \ln Z$ in the thermodynamic limit, where N_s denotes the number of sites on the lattice.

3. Some basic properties

We begin by discussing the phase boundaries of the model as a function of complex temperature, i.e. the locus of points across which the free energy is non-analytic. The physical phases of the model include the phase where the Z_2 symmetry is realized explicitly, namely, the paramagnetic (PM) phase, and also, for dimension greater than the lower critical

dimensionality (i.e. $d \geq 2$, for integer d), a phase where the Z_2 symmetry is spontaneously broken with long-range ferromagnetic (FM) order, i.e. a non-zero spontaneous (uniform) magnetization, M . For the lattices considered here which are bipartite and hence involve no frustration for antiferromagnetic (AFM) ordering, there is also a phase with AFM long-range order, i.e. a non-zero staggered magnetization, M_{st} . As one can see from table 1, of the three heteropolygonal lattices considered here, only the $(4 \cdot 8^2)$ lattice is bipartite. One defines the complex-temperature extensions of the physical phases by analytic continuation in K or an equivalent variable such as v , z , or u . There are, in general, also complex-temperature phases which have no overlap with any physical phase. As in our earlier work, we label these as O phases (where O denotes ‘other’), including subscripts to distinguish them where there are several. In cases where one O phase is precisely the complex conjugate of another, we label the one with $\text{Im}(z) \geq 0$ by O (with subscript where necessary) and its complex conjugate by O^* . (From equation (2.3), it follows that in the v plane, the corresponding O and O^* phases have $\text{Im}(v) \leq 0$ and $\text{Im}(v) \geq 0$, respectively.)

As noted in [9], there is an infinite periodicity in complex K under the shift $K \rightarrow K + n\pi$, where n is an integer, and, for lattices with even coordination number q , also the shift $K \rightarrow (2n+1)i\pi/2$, as a consequence of the fact that the spin–spin interaction $\sigma_n \sigma_{n'}$ in \mathcal{H} is an integer. In particular, there is an infinite repetition of phases as functions of complex K . These repeated phases are reduced to a single set by using the variables v , z or u , owing to the symmetry relation $K \rightarrow K + n\pi \Rightarrow \{v \rightarrow v, z \rightarrow z, u \rightarrow u\}$. It is thus convenient to use these variables here.

As we have discussed in our earlier papers [11, 12], the equations for the locus of points where the free energy is non-analytic also serve to define the boundaries of the complex-temperature phases of the model. Some of the loci of points where the free energy is non-analytic do not actually separate any phases, but rather are arcs or line segments protruding into various phases. In passing we note that the free energy is, of course, also trivially non-analytic at $K = \pm\infty$, i.e. $v = \pm 1$ or $z = 0, \infty$. This is obvious from (2.1) and (2.2). Because these points are isolated, they do not separate any complex-temperature phases and hence will not be important here.

Before proceeding, we list some theorems. Although these are elementary, it will be useful to record them here for our later discussion of the complex-temperature phase diagrams. Some of the theorems will be given in greater generality than is needed here.

Theorem 1. Consider the (spin- $\frac{1}{2}$, zero-field) Ising model on an arbitrary lattice. The loci of points in the complex z and v planes where the free energy of the Ising model is non-analytic are symmetric under complex conjugation, i.e. under reflection about the $\text{Im}(z) = 0$ and $\text{Im}(v) = 0$ axes, respectively. Hence the same is true of the complex-temperature phase boundaries in these variables. The same is also true of the zeros of the partition function on finite lattices. This follows from the well known fact that the partition function is a generalized polynomial in z with real coefficients. (Here, a ‘generalized’ polynomial in the variable ζ is defined as a finite sum of integral powers of ζ , where negative as well as positive powers are allowed.) This theorem can be extended in two ways. First, the theorem actually applies not just for the case of zero external field, but also for the case of non-zero (real) magnetic field. One can also show that it is true for pure imaginary h . Secondly, one can straightforwardly generalize theorem 1 to the case of the spin- s Ising model.

Theorem 2. For the (spin- $\frac{1}{2}$, zero-field) Ising model, if and only if the lattice has even coordination number $q = 2r$, the complex-temperature phase diagram is invariant under the transformation $z \rightarrow -z$. The same is true of the zeros of the partition function for finite

lattices. This follows by explicit calculation of the partition function for finite lattices. For odd (even) q , Z is a generalized polynomial in z (in $u = z^2$). Thus, for lattices with even q , a more compact way to display the complex-temperature phase diagram is in the complex u plane.

Theorem 3. For the (spin- $\frac{1}{2}$, zero-field) Ising model, if and only if the lattice is bipartite, the complex-temperature phase diagram is invariant under the transformation $z \rightarrow 1/z$ ($u \rightarrow 1/u$ if also q is even). The same is true of the zeros of the partition function for finite lattices. This is proved using the well known mapping involving the reversal of signs of spins on one of the two sublattices, together with $J \rightarrow -J$, under which Z is invariant.

Theorem 4. In the z plane, the zeros (and any divergences) of the spontaneous magnetization M occur at either real values or at complex conjugate pairs of values. This is a corollary of the generalization of theorem 1 to the case of non-zero (real) external field h . Since $M = \lim_{H \rightarrow 0} \partial M / \partial h$, this generalization of theorem 1 implies that $M(z)^* = M(z^*)$. Hence, in particular, the set of zeros (and any divergences) of M as a function of z is invariant under $z \rightarrow z^*$.

Theorem 5. On a bipartite lattice, in the $w = 1/z$ plane, the zeros (and any divergences) of the spontaneous staggered magnetization M_s , occur at either real values or at complex conjugate pairs of values. This is a corollary of theorem 4. Note that

$$M_{st}(w) = M(z \rightarrow w). \quad (3.1)$$

Theorem 6. For lattices with odd coordination number q , the zero-field partition function Z of the (spin- $\frac{1}{2}$) Ising model vanishes at $z = -1$, and the free energy contains a negatively divergent singularity at this point.

This theorem is proved as follows. From the definition of the partition function and of K , we have

$$Z = \sum_{\{\sigma_n\}} \exp\left(K \sum_{\langle nn' \rangle} \sigma_n \sigma_{n'}\right). \quad (3.2)$$

Now, in general, for each bond $\langle nn' \rangle$, since $\sigma_n \sigma_{n'} = \pm 1$, it follows that

$$e^{K\sigma_n \sigma_{n'}} = \cosh K + \sigma_n \sigma_{n'} \sinh K. \quad (3.3)$$

The K values corresponding to $z = \lim_{\epsilon \rightarrow 0} (-1 \pm \epsilon)$ (where ϵ denotes a small real number) are $K = -\frac{1}{2} \lim_{\epsilon \rightarrow 0} \ln(-1 \pm \epsilon) = -\frac{1}{2}(\pm i\pi + 2ni\pi)$, where we follow the usual convention of taking the branch cut for $\log z$ to lie along the negative real z axis, and n indexes the Riemann sheet of the logarithm. To minimize unimportant minus signs, we consider $z = \lim_{\epsilon \rightarrow 0} (-1 - \epsilon)$ and take the principal Riemann sheet of the log, $n = 0$; then $K = i\pi/2$. Substituting this into (3.3), we have

$$e^{(i\pi/2)\sigma_n \sigma_{n'}} = i\sigma_n \sigma_{n'} \quad (3.4)$$

so that

$$Z = \sum_{\{\sigma_n\}} \left(\prod_{\langle nn' \rangle} i\sigma_n \sigma_{n'} \right). \quad (3.5)$$

Since the lattice has coordination number q , in this product over all bonds, the σ_n for each site n appears q times, and hence (3.5) can be rewritten as a product over all sites:

$$Z = i^{N_t} \sum_{\{\sigma_n\}} \left(\prod_n \sigma_n^q \right). \quad (3.6)$$

Evaluating the summation over each spin, we have

$$Z = i^{N_s} [(+1)^q + (-1)^q]^{N_s}. \quad (3.7)$$

Evidently, for odd q , the summation over $\sigma_n = \pm$ on each site yields 0, and hence $Z = 0$, so that the free energy is negatively divergent at this point. \square

Among the lattices considered here, the hexagonal, $(3 \cdot 12^2)$, and $(4 \cdot 8^2)$ ones have odd q (in each case, $q = 3$), so that theorem 6 implies that the respective free energy f for each has a divergent singularity at $z = -1$.

From equation (3.7) in the proof of theorem 6, it is immediately evident that for the (spin- $\frac{1}{2}$) Ising model on a lattice of even $q = 2r$, the value of the partition function on a finite lattice with periodic boundary conditions (and hence the relation $N_t = (q/2)N_s$) is

$$Z(z = -1; q = 2r) = i^{rN_s} 2^{N_s} \quad (3.8)$$

while the (reduced) free energy satisfies

$$f(z = -1; q = 2r) = r \ln i + \ln 2 \quad (3.9)$$

(independent of boundary conditions, since these do not affect the thermodynamic limit). In equation (3.9), $\ln i = i\pi/2 + 2\pi in$, where n labels the Riemann sheet of the log.

The points across which the free energy is non-analytic are related to the zeros of the partition function. A fundamental question concerns whether these points (apart from the trivial ones at $K = \pm\infty$ and, for odd q , at $z = -1$ as proved in theorem 6) lie on curves (including line segments) in the z (or equivalently, v) plane, or whether they lie in areas. For homopolygona 2D lattices with isotropic spin-spin exchange couplings, these points do lie on curves. (There is also numerical evidence for this in the case of 3D lattices [8].) It is also well known that for 2D homopolygona lattices with anisotropic couplings, these points lie, in general, in areas rather than on curves [18]. It is worthwhile to investigate this question for heteropolygona lattices, and we shall do so, as part of our general determination of the complex-temperature phase diagrams. Indeed, one of our interesting results will be the finding that even for isotropic spin-spin couplings, the zeros do not always lie on curves in the case of heteropolygona lattices. We shall give a simple explanation of this finding below.

We now proceed with our analyses.

4. $(3 \cdot 6 \cdot 3 \cdot 6)$ lattice

The (zero-field) free energy of the Ising model on the $(3 \cdot 6 \cdot 3 \cdot 6)$ (kagomé) lattice with equal spin-spin couplings was first calculated explicitly by Kano and Naya [19]. The result is

$$f_{kag} = \ln 2 + \frac{1}{6} \int_{-\pi}^{\pi} \int_{-\pi}^{\pi} \frac{d\theta_1 d\theta_2}{(2\pi)^2} \ln \left\{ \frac{1}{4} [(C^3 + S^3)^2 + 3C^2 - 2CS^2(C + S)P(\theta_1, \theta_2)] \right\} \quad (4.1)$$

where

$$P(\theta_1, \theta_2) = \cos(\theta_1) + \cos(\theta_2) + \cos(\theta_1 + \theta_2). \quad (4.2)$$

As was the case with the homopolygona lattices, the connected locus of points across which the free energy is non-analytic is the set of points for which the logarithm in the integral of (4.1) vanishes. These are also the zeros of the partition function. In terms of the variable u , this vanishing condition is the equation

$$(21u^4 + 24u^3 + 18u^2 + 1) - 4u(1+u)(1-u)^2 x = 0 \quad (4.3)$$

where x represents $P(\theta_1, \theta_2)$ and takes values in the range

$$-\frac{3}{2} \leq x \leq 3. \quad (4.4)$$

For $x = 3$, there is a double real root at $u_{c,kag}$, where

$$u_{c,kag} = -1 + \frac{2}{\sqrt{3}} \simeq 0.15470054\dots \quad (4.5)$$

and another double real root at $-1/(3u_{c,kag}) = -1 - 2/\sqrt{3}$. As indicated in the notation, $u_{c,kag}$ is the physical critical point separating the FM and PM phases. As x decreases from 3 in the range $-1 < x < 3$, each of these splits into two pairs, which trace out the curves in figure 5(a). For $x = -1$, these rejoin in conjugate double roots at the multiple or intersection points u_k and u_k^* , where

$$u_k = \frac{1}{5}(-1 + 2i) = 5^{-1/2}e^{i\theta_k} \quad (4.6)$$

with

$$\theta_k = \pi - \arctan(2) \simeq 116.57^\circ. \quad (4.7)$$

As in our earlier papers [11, 12], we denote these as multiple points, following the technical terminology of algebraic geometry, according to which a multiple point of an algebraic curve is a point where two or more branches (arcs) of the curve cross [20]. We shall use the words ‘intersection point’ and ‘multiple point’ synonymously here. The corresponding numerical values of $z_k = \pm 5^{-1/4}e^{i\theta_k/2}$ are

$$z_k = \pm(0.3515776 + 0.5688645i). \quad (4.8)$$

Finally, as x decreases from -1 toward $-\frac{3}{2}$, these split again, with one root moving away from u_k upward along an arc of the circle defined by

$$|u - \frac{1}{3}| = \frac{2}{3} \quad (4.9)$$

toward the endpoint of this arc on the positive imaginary axis, given by

$$u_e = \frac{i}{\sqrt{3}} \quad (4.10)$$

the conjugate root moving down from u_k^* on the circle (4.9) toward u_e^* , and the other two roots moving along the circle (4.9) toward the real axis. Finally, at $x = -\frac{3}{2}$, two roots occur at the endpoints u_e , u_e^* , and there is a double root at the point $u = u_\ell \equiv -\frac{1}{3}$.

In terms of the commonly used variable z , the complex phase diagram is shown in figure 5(b). From the fact that the equation (4.3) for the locus of points where f is non-analytic is symmetric under $z \rightarrow -z$, it follows that the phase diagram in the z plane has this symmetry also. The physical critical point is $z_c = (-1 + 2/\sqrt{3})^{1/2} \simeq 0.393320\dots$. The boundary of the complex-temperature FM phase crosses the real z axis at the points $\pm z_c$. Corresponding to the intersection point u_k and its conjugate there are four intersection points $z_k = 5^{-1/4}e^{i\theta_k/2}$, $-z_k$, and $\pm z_k^*$. The outermost points on the boundaries of the O phases are given by $z_o = i|(-1 - 2/\sqrt{3})|^{1/2}$ and z_o^* .

Finally, by a conformal mapping or directly from (4.1), one can also determine the corresponding loci of points in the v plane. The equation for this locus of points is

$$1 - 4v + 10v^2 - 16v^3 + 22v^4 - 16v^5 + 10v^6 - 4v^7 + v^8 - 2v^2(1-v)^2(1+v^2)x = 0. \quad (4.11)$$

Up to an overall factor of v^{-8} , this equation is invariant under the transformation $v \rightarrow 1/v$. This together with the reality of the coefficients implies that the locus of solutions is invariant

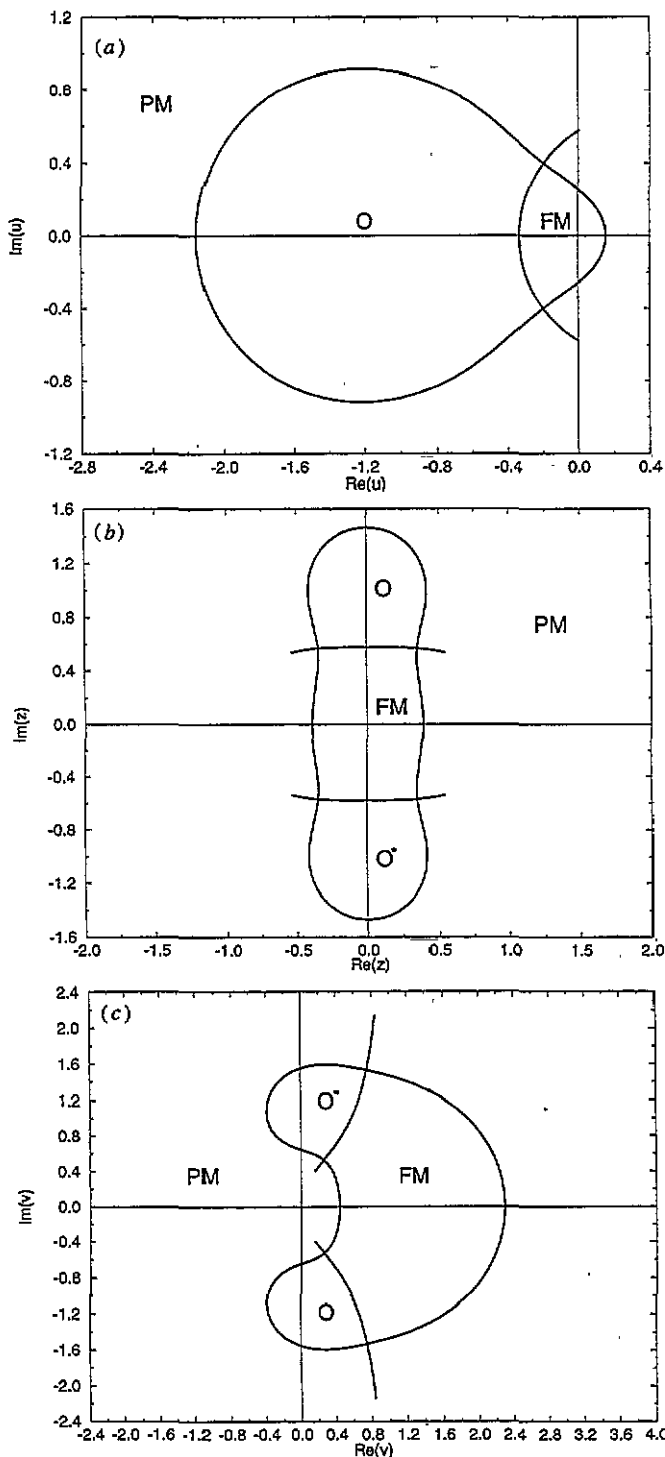


Figure 5. Complex-temperature phase diagram for the Ising model on the $3 \cdot 6 \cdot 3 \cdot 6$ (kagomé) lattice, in the variable (a) u , (b) z , (c) v .

under (i) $v \rightarrow v^*$ and (ii) $v \rightarrow 1/v$. This locus is shown in figure 5(c). The complex-temperature phases are marked on this figure and consist of the PM and FM phases, together

with two O phases which are related to each other by complex conjugation. From the value of u_c or z_c and the relation (2.3), it follows that the critical value of v is

$$v_{c,kag} = \frac{1}{2}(1 + 3^{1/2}) \left[1 - (2\sqrt{3} - 3)^{1/2} \right] \simeq 0.43542054 \dots \quad (4.12)$$

One sees that the kidney-shaped curve enclosing the FM and two O phases crosses the real- v axis at the points v_c and $1/v_c \simeq 2.29663 \dots$. The four intersection points of the kidney-shaped curve and the arcs are given by $v_k = (1 - z_k)/(1 + z_k)$, its complex conjugate, v_k^* , and their two reciprocals, $1/v_k$ and $1/v_k^*$. Similarly, the four endpoints of the arcs are given by $v_e = (1 - z_e)/(1 + z_e)$, v_e^* , $1/v_e$, and $1/v_e^*$. We find that the inner endpoints of the arcs are the same distance from the origin as the physical critical point, i.e. $|v_e| = v_c$.

The phase structure consists of PM and FM phases, but, as is well known, no AFM phase because of the frustration associated with AFM ordering. These characteristics are the same as those for the (isotropic) Ising model on the triangular lattice. In addition, figures 5(a) and (b) show two complex-temperature phases denoted O and O* which have no overlap with any physical phase. In the u variable (see figure 5(c)), these are mapped onto a single O phase. In our previous work, we found O phases for the square and triangular (but not hexagonal) lattices, in the v and z plane. However, for both the square and triangular lattices, each point z in the O phase was just the negative of a corresponding point in the complex PM phase, and hence under the mapping from the z to u plane, these were mapped to the same point, which could be considered just the complex PM phase. We find for the kagomé lattice a new property, namely, a distinct O phase which persists even in the u plane.

The spontaneous magnetization cannot be written in the same form $M = (1 - (k_{<,\Lambda})^2)^{1/2}$ as for the regular unipolygonal lattices $\Lambda = \text{sq, tri, hex}$. Rather, it has the following form in the FM phase (and vanishes identically elsewhere) [21]:

$$M_{kag} = \frac{(1 + 3u)^{1/2}(1 - u)^{1/2}}{(1 + u)} (1 - (k_{<,kag})^2)^{1/8} \quad (4.13)$$

where

$$k_{<,kag} = \frac{2^{7/2}u^{3/2}(1 + u)^{3/2}(1 + 3u^2)^{1/2}}{(1 - u)^3(1 + 3u)} \quad (4.14)$$

i.e.

$$M_{kag} = \frac{(1 - 6u - 3u^2)^{1/8}(1 + 2u + 5u^2)^{3/8}(1 + 3u)^{1/4}}{(1 - u)^{1/4}(1 + u)} \quad (4.15)$$

These formulae may be analytically continued through the complex-temperature extension of the FM phase. Note the factorizations $1 - 6u - 3u^2 = (1 - u/u_{c,kag})(1 + 3u_{c,kag}u)$ and $1 + 2u + 5u^2 = (1 - u/u_k)(1 - u/u_k^*)$.

From equation (4.15) and our determination of the complex-temperature FM phase in which the analytic continuation of this formula holds, it follows that besides the well known fact that M_{kag} vanishes continuously at the physical critical point u_c , with exponent $\beta = \frac{1}{8}$, it also vanishes continuously at the complex-temperature points $u_\ell = -\frac{1}{3}$ with exponent

$$\beta_{kag,\ell} = \frac{1}{4} \quad (4.16)$$

and at the points u_k and u_k^* with exponent

$$\beta_{kag,k} = \frac{3}{8} \quad (4.17)$$

Elsewhere along the boundary of the complex-temperature FM phase, M vanishes discontinuously. One may observe that the expression for M has an apparent zero at

Table 2. Points at which M and M_{st} vanish continuously (or diverge) for the $(3 \cdot 6 \cdot 3 \cdot 6)$ (kagomé), $(3 \cdot 12^2)$, and $(4 \cdot 8^2)$ (bathroom tile) lattices, together with the three homopolygona 2D lattices, for comparison. Under the M and M_{st} columns, an entry marked — means that the point cannot be reached from within the FM and AFM phases, respectively. The symbol N means that the model has no AFM phase. (mp) means a multiple (= intersection) point through which two or more phase boundary arcs pass. See the text for further discussions.

Λ	z	Value	M	M_{st}	β	Adj. phases
sq (4^4)	z_c	$\sqrt{2} - 1$	zero	—	1/8	FM-PM
	$-z_c$	$-(\sqrt{2} - 1)$	zero	—	1/8	O-FM
	z_c^{-1}	$\sqrt{2} + 1$	—	zero	1/8	PM-AFM
	$-z_c^{-1}$	$-(\sqrt{2} + 1)$	—	zero	1/8	AFM-O
	z_s, z_s^*	$\pm i$	zero	zero	1/4	O-FM-PM-AFM (mp)
tri (3^6)	z_c	$1/\sqrt{3}$	zero	N	1/8	FM-PM
	$-z_c$	$-1/\sqrt{3}$	zero	N	1/8	O-FM
	z_s, z_s^*	$\pm i$	zero	N	3/8	O-PM-FM (mp)
	z_e, z_e^*	$\pm i/\sqrt{3}$	div.	N	-1/8	Protrusion in FM
hex (6^3)	z_c	$2 - \sqrt{3}$	zero	—	1/8	FM-PM
	z_c^{-1}	$2 + \sqrt{3}$	—	zero	1/8	PM-AFM
	z_s, z_s^*	$\pm i$	zero	zero	3/8	FM-PM-AFM (mp)
		-1	div.	div.	-1/4	AFM-FM
$(3 \cdot 6 \cdot 3 \cdot 6)$	z_c	$(-1 + 2/\sqrt{3})^{1/2}$	zero	N	1/8	FM-PM
	$-z_c$	$-(1 + 2/\sqrt{3})^{1/2}$	zero	N	1/8	PM-FM
	$\pm z_k$	$\pm i/\sqrt{3}$	zero	N	1/4	FM-O, FM-O*
	$\pm z_k^*$	equation (4.8)	zero	N	3/8	FM-PM-O (mp)
$(3 \cdot 12^2)$	$z_c = z_{a+}$	equations (5.5) and (5.6)	zero	N	1/8	FM-PM
	z_{a-}	equations (5.5) and (5.7)	zero	N	1/8	PM-FM
	$\pm i/\sqrt{3}$	zero	N	1/4	FM-O(*)	
	$\pm i$	zero	N	3/8	FM-PM-O(*) (mp)	
	z_r, z_r^*	$(1 \pm 2i)/5$	zero	N	3/8	FM-PM-O(*) (mp)
		-1	div.	N	-1/2	Interior of FM
$(4 \cdot 8^2)$	$z_c = z_{1+}$	equations (6.15) and (6.20)	zero	—	1/8	FM-PM (mp; tn)
	$(z_{1-})^{-1}$	equations (6.17) and (6.21)	zero	—	1/8	O ₁ -FM (mp; tn)
	$z_{3-}^*, z_{3,-}$	equations (6.19) and (6.25)	zero	—	1/8	FM-O ₂ ^(*) (mp)
	$z_c^{-1} = (z_{1+})^{-1}$	equations (6.17) and (6.20)	—	zero	1/8	PM-AFM (mp; tn)
	z_{1-}	equations (6.15) and (6.21)	—	zero	1/8	AFM-O ₁ (mp; tn)
	z_{3+}, z_{3+}^*	equations (6.19) and (6.24)	—	zero	1/8	AFM-O ₃ ^(*) (mp)

$u = -1/(3u_{kag,c}) = -1 - 2/\sqrt{3} \simeq -2.1547$ (the point where the left boundary in figure 5(a) crosses the real u axis) and apparently divergences at $u = 1$ and $u = -1$; however, none of these singularities actually occurs since all of these points are outside of the complex-temperature extension of the FM phase where expression (4.15) holds. This is clear from the phase diagram in figure 5(a).

The characteristics of the points where M vanishes continuously are listed in table 2, which includes a comparison with the three 2D homopolygona lattices. The column marked z gives the symbol, if one was assigned, for each of the zeros (or divergences) in the uniform (and, where relevant, staggered) magnetization. The column marked ‘Value’ lists either the analytic expression or, where this is too long to fit into the space, a reference to the equation(s) where this is given in the text. The column marked ‘Adj. phases’ lists the phases which are adjacent to the given point. For conciseness, some lines list a point and its complex conjugate together; in these cases, the notation O^(*) in the adjacent phase

column means O for the first point and O* for its complex conjugate. One may recall that the divergence in M for the triangular lattice occurs at $z = \pm 1/\sqrt{3}$ which are the endpoints of two line segments protruding into the complex-temperature FM phase; this is indicated in the table by the notation 'protrusion in FM'. Other notation is explained in the table caption.

In table 2, for comparative purposes, we describe the characteristics on all of the lattices in terms of the z plane; however, we note that for lattices with even coordination number, since quantities can be expressed solely in terms of $u = z^2$, a more compact way of depicting the phase diagram is in terms of the u plane.

5. $(3 \cdot 12^2)$ lattice

The (zero-field) free energy for the $(3 \cdot 12^2)$ lattice with isotropic couplings was given implicitly in [22, 16]. For various generalizations to unequal couplings, the free energy was given in [23, 24]. Evaluating some intermediate expressions and performing some algebra, we obtain the explicit expression, in terms of z (and $K = -\frac{1}{2} \ln z$),

$$f_{3-12} = \frac{3}{2}K + \frac{1}{2} \ln(1+z) + \frac{1}{12} \int_{-\pi}^{\pi} \int_{-\pi}^{\pi} \frac{d\theta_1 d\theta_2}{(2\pi)^2} \ln[A_{3-12} + B_{3-12}P(\theta_1, \theta_2)] \quad (5.1)$$

where

$$A_{3-12} = 1 - 6z + 24z^2 - 42z^3 + 66z^4 - 42z^5 + 48z^6 - 6z^7 + 21z^8 \quad (5.2)$$

$$B_{3-12} = -2z(1-z+2z^2)(1+z)(1-z)^4. \quad (5.3)$$

Since this lattice has odd coordination number $q = 3$, theorem 6 states that, in addition to the trivial singularities at $K = \pm\infty$, i.e. $z = 0, \infty$, the free energy f has a singularity at $z = -1$. This is evident in (5.1). If one takes the branch cut for the logarithm to extend from $z = -1$ to $z = -\infty$, then as one approaches $z = -1$ from the direction of the origin, f becomes negatively infinite. In the case of the honeycomb lattice, as was noted in [12], this point lies on the continuous locus of points where the argument of the logarithm in the integrand analogous to (5.1) vanishes. However, in contrast to the honeycomb lattice, for the $(3 \cdot 12^2)$ and $(4 \cdot 8^2)$ lattices, this singularity is an isolated one. Aside from these isolated singular points, the free energy also has non-analyticities which arise from the vanishing of the argument of the logarithm inside the integral in equation (5.1). The condition for this vanishing is

$$A_{3-12} + B_{3-12}x = 0 \quad (5.4)$$

where x represents $P(\theta_1, \theta_2)$ as given above in (4.2). This yields the curves shown in figure 6(a) (see also the corresponding curves in the v plane in figure 6(b)). As marked there, these curves serve to bound the complex-temperature extensions of the FM and PM phases and also two phases which have no overlap with any physical phase, and are labelled O and O*. The border of the complex FM phase crosses the real z axis at the points

$$z_{a\pm} = \frac{1}{2} \left[-(\sqrt{3} + 1) \pm \left(4 + \frac{10}{3}\sqrt{3} \right)^{1/2} \right] \quad (5.5)$$

with numerical values

$$z_{a+} = 0.19710468\dots \quad (5.6)$$

$$z_{a-} = -2.9291555\dots \quad (5.7)$$

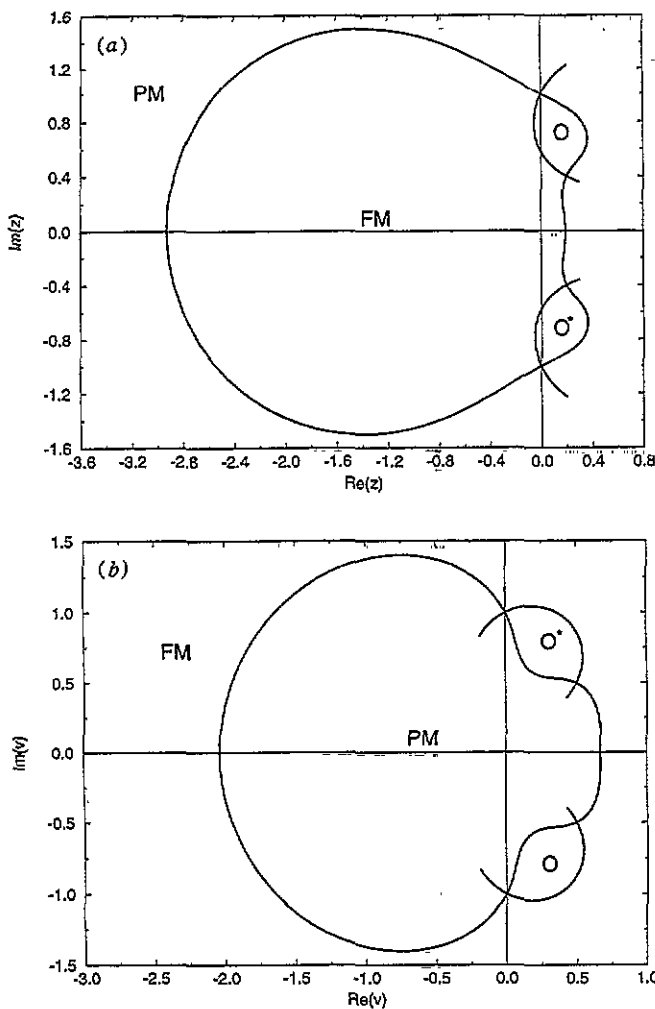


Figure 6. Complex-temperature phase diagram for the Ising model on the $3 \cdot 12^2$ lattice, in the variable (a) z , (b) v .

The physical critical point of the model is $z_{c,3-12} = z_{a+}$. The intersection points nearest to the real z axis are given by z_r and z_r^* , where

$$z_r = \frac{1 - 2i}{5} = 5^{-1/2} e^{i\theta_k} \quad (5.8)$$

where θ_k was given above in (4.7) (for certain formally analogous points in the u plane). The intersection points farther out from the real z axis occur at $z = \pm i$. For $x = 3$, there are four double roots at z_{a+} , z_{a-} , z_b , and z_b^* , where

$$z_b = \frac{1}{2} \left[(\sqrt{3} - 1) + (4 - \frac{10}{3}\sqrt{3})^{1/2} \right] \simeq 0.366\,025\,40 + 0.665\,864\,61i. \quad (5.9)$$

As can be seen from figure 6(a), the points z_b and z_b^* lie roughly at the centres of the outer boundaries of the respective O and O^* phases. As x decreases from 3 in the range $-1 \leq x \leq 3$, these double roots split apart into pairs the members of which move away from these four points, tracing the curves shown in figure 6(a). At $x = -1$, these points

rejoin at the four intersection points $z = \pm i$ and $z = z_r$ and z_r^* . As x decreases further in the range $-\frac{3}{2} \leq x \leq -1$, these four double roots split again, with two of the roots moving toward each other on the arc forming the inner boundary of the O phase adjacent to the FM phase, and similarly with two other roots on the inner boundary of the O* phase, while the other four roots move outward away from the origin along the two arcs and their complex conjugates. Finally, at $x = -\frac{3}{2}$, two pairs of roots on the inner arcs join to form double roots at $z = \pm i/\sqrt{3}$, while the four outer roots reach the endpoints of the arcs. These endpoints are as follows:

$$z_{e\pm} = \frac{1}{2} [e^{i\pi/3} \pm (e^{2i\pi/3} - (\frac{4}{3})\sqrt{3}e^{i\pi/6})^{1/2}] \quad (5.10)$$

with the values

$$z_{e+} \approx 0.295\ 567\ 91 - 0.358\ 868\ 9i \quad (5.11)$$

$$z_{e-} \approx 0.204\ 432\ 09 + 1.224\ 894\ 3i \quad (5.12)$$

are, respectively, the endpoints of the upper parts of the arcs in the upper- and lower-half z plane. Their complex conjugates z_{e+}^* and z_{e-}^* form the endpoints of the lower parts of these arcs.

From implicit expressions given in [23], we can express the spontaneous magnetization as

$$M_{3-12} = \frac{(1 - 6z + 6z^2 - 6z^3 - 3z^4)^{1/8}(1 + 3z^2)^{1/4}(1 + z^2)^{3/8}(1 - 2z + 5z^2)^{3/8}}{(1 - z)(1 + z)^{1/2}(1 - z + 2z^2)}. \quad (5.13)$$

By analytic continuation, this expression holds throughout the complex-temperature extension of the FM phase, which we have determined, as shown in figure 6(a). Note the factorization

$$1 - 6z + 6z^2 - 6z^3 - 3z^4 = -3(z - z_{a+})(z - z_{a-})(z - z_b)(z - z_b^*). \quad (5.14)$$

Moreover, similar to another formula above (for u rather than z), we have the factorization $1 - 2z + 5z^2 = (1 - z/z_r)(1 - z/z_r^*)$. Finally, we note that $1 - z + 2z^2 = 2(z - z_o)(z - z_o^*)$, where

$$z_o = \frac{1}{4}(1 + i\sqrt{7}) = 0.25 + i0.661\ 437\ 83\dots \quad (5.15)$$

These points z_o and z_o^* lie in the middle of the two complex conjugate O phases. Thus, M_{3-12} vanishes continuously at the eight points z_{a+} , z_{a-} , $\pm i/\sqrt{3}$, $\pm i$, z_r , and z_r^* . In table 2 we list these zeros, together with the corresponding exponents β and the phases which are adjacent at each point. Elsewhere along the boundary of the complex-temperature FM phase, M vanishes discontinuously. M_{3-12} also has a divergence at the isolated point $z = -1$ in the interior of the complex-temperature FM phase, where the free energy itself is also singular. In addition to these actual singularities, the formal expression (5.13) has apparent zeros at the points z_{b+} , $z_{b-} = z_{b+}^*$, z_o , and z_o^* , but these are not zeros of the actual magnetization, since these points cannot be reached from within the complex-temperature FM phase where the expression (5.13) holds. As one can see from figure 6(a), z_b lies on the boundary separating the O and PM phase, and similarly z_b^* lies on the boundary between the O* and PM phase. The points z_o and z_o^* lie in the interior of the O and O* phases, respectively.

6. $(4 \cdot 8^2)$ lattice

In contrast to the $(3 \cdot 6 \cdot 3 \cdot 6)$ and $(3 \cdot 12^2)$ lattices, the $(4 \cdot 8^2)$ (bathroom tile) lattice is bipartite, and the physical phase diagram consists of a PM, FM, and also AFM phase. One way to obtain the (zero-field) free energy is from the free energy for the dual $[4 \cdot 8^2]$ (Union Jack) lattice. An explicit calculation of the latter for the case of equal spin-spin couplings was given in [25]. (See also the remarks in [15]; for the Union Jack lattice with general couplings, which we shall not need here, see also [26] and [27].) Using this duality relation, one easily obtains the free energy for the $(4 \cdot 8^2)$ lattice, in terms of z (and $K = -\frac{1}{2} \ln z$), as follows:

$$f_{4 \cdot 8} = \frac{3}{2} K + \frac{1}{2} \ln(1+z) + \frac{1}{8} \int_{-\pi}^{\pi} \int_{-\pi}^{\pi} \frac{d\theta_1 d\theta_2}{(2\pi)^2} \ln[A_{4 \cdot 8}(z) + B_{1;4 \cdot 8}(z)(\cos \theta_1 + \cos \theta_2) + B_{2;4 \cdot 8}(z) \cos \theta_1 \cos \theta_2] \quad (6.1)$$

where

$$A_{4 \cdot 8}(z) = (1+z^2)^2(1-4z+10z^2-4z^3+z^4) \quad (6.2)$$

$$B_{1;4 \cdot 8}(z) = 2z(1-z)^3(1+z)(1+z^2) \quad (6.3)$$

$$B_{2;4 \cdot 8}(z) = -4z^2(1-z)^4. \quad (6.4)$$

In addition to the trivial singularities at $K = \pm\infty$, i.e. $z = 0, \infty$, and the additional isolated singularity at $z = -1$, the free energy has non-analyticities where the argument of the logarithm in the integrand of (6.1) vanishes. These are given by the equation

$$A_{4 \cdot 8}(z) + B_{1;4 \cdot 8}(z)(\cos \theta_1 + \cos \theta_2) + B_{2;4 \cdot 8}(z) \cos \theta_1 \cos \theta_2 = 0. \quad (6.5)$$

We find that the locus of points which are solutions to this equation fall, in general, into areas rather than curves, in the z or, equivalently, the v planes. These areas degenerate into points at certain special locations. In figure 7(a) we show the solution to (6.5) in the z plane, for a grid of values of θ_1 and θ_2 . Because of the finite grid of values of θ_1 and θ_2 used to make the plots, the zeros show a striped structure in certain regions; it is understood that in the limit where the aforementioned grid of values of θ_1 and θ_2 becomes infinitely fine, these stripes would merge into coherent areas; the boundaries of these areas are easily inferred from the plot. The phases include the complex-temperature extensions of the physical FM, PM, and AFM phases, as marked, together with five phases which have no overlap with any physical phases, labelled O_1 , O_2 , O_2^* , O_3 and O_3^* . The rest of the z plane involves various continuous regions of points where the free energy is non-analytic (forming the thermodynamic limits of zeros of the partition functions for finite lattices). We shall discuss the special locations where the areas of zeros of the partition function degenerate into points below, in conjunction with an analysis of the spontaneous uniform and staggered magnetizations. The corresponding diagram in the v plane is shown in figure 7(b). As in figure 7(a), because of the finite grid of values of θ_1 and θ_2 used to make the plot, the zeros exhibit a striped or dotted structure in certain regions; again, it is understood that for a dense set of values of θ_1 and θ_2 , the zeros in these regions form a continuous set.

To our knowledge, this finding constitutes the first known case of an Ising model with isotropic spin-spin couplings, where the non-analyticities of the free energy (aside from the trivial ones at $K = \pm\infty$ and, for odd q , at $z = -1$, as proved in theorem 6) form a two-dimensional, rather than one-dimensional, algebraic variety, i.e. lie in areas rather than on curves (including line segments). It is easy to understand the basis for this result. The locus of points at which the free energy is non-analytic (aside from the above-mentioned trivial singularities) is determined by the condition that in the integral occurring in the free energy,

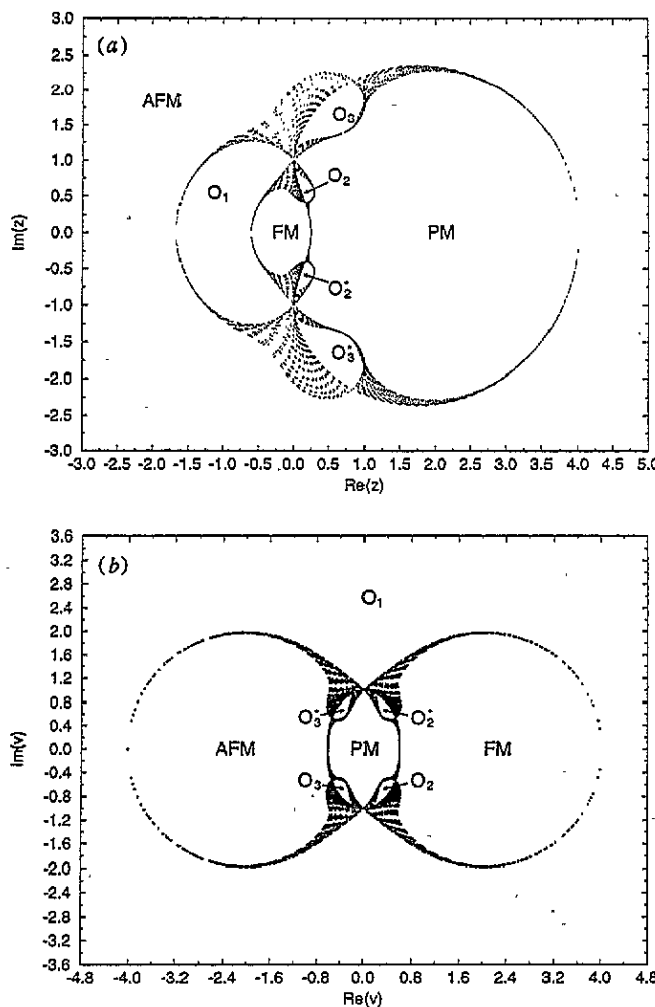


Figure 7. Complex-temperature phase diagram for the Ising model on the $4 \cdot 8^2$ (bathroom tile) lattice, in the variable (a) z , (b) v .

the expression in the argument of the logarithm vanishes. For homopolygona lattices, this expression reduces to the equation

$$A_\Lambda(z) + B_\Lambda(z)x = 0 \quad (6.6)$$

for isotropic spin-spin couplings, where x represents the function $P(\theta_1, \theta_2) = \cos \theta_1 + \cos \theta_2$ for the square lattice and $P(\theta_1, \theta_2) = \cos \theta_1 + \cos \theta_2 + \cos(\theta_1 + \theta_2)$ for the triangular and hexagonal (honeycomb) lattices. (Thus for the square lattice, $-2 \leq x \leq 2$, while for the triangular and hexagonal lattices, $-\frac{3}{2} \leq x \leq 3$.) The solutions to (6.6) form a one-dimensional algebraic variety, specifically, algebraic curves (including possible line segments). In contrast, for unequal spin-spin exchange constants J_i , where $i = 1, 2$ for the square lattice, and $i = 1, 2, 3$ for the triangular and hexagonal lattices, the condition for the argument of the logarithm in the integrand to vanish is of the form

$$A_{sq} + B_{sq;1} \cos \theta_1 + B_{sq;2} \cos \theta_2 = 0 \quad (6.7)$$

for the square lattice, and

$$A_\Lambda + B_{\Lambda;1} \cos \theta_1 + B_{\Lambda;2} \cos \theta_2 + B_{\Lambda;3} \cos(\theta_1 + \theta_2) = 0 \quad (6.8)$$

for the triangular and hexagonal lattices, where in each case, the various A and B functions depend on the z_i , with $z_i = e^{-2K_i}$ and $K_i = \beta J_i$. Now let the (anisotropic) ratios of the J_i 's be fixed. Then equations (6.7) and (6.8) depend on two independent real (periodic) variables, θ_1 and θ_2 . It follows that the solutions, in general, form a two-dimensional algebraic variety, specifically areas (which may degenerate to points at special values of z).

The heteropolygona lattices $(3 \cdot 6 \cdot 3 \cdot 6)$ and $(3 \cdot 12^2)$ are similar to the homopolygona lattices in this respect, i.e. if the spin-spin couplings on each bond are equal, then the condition for the argument of the logarithm in the integrand to vanish is of the form (6.6). However, as is evident from (6.1), this is not the case for the $(4 \cdot 8^2)$ lattice. That is, even if the spin-spin couplings are equal for each bond, the condition for the vanishing of the argument of the logarithm in (6.1) is of the form (6.5), which depends on two independent real (periodic) variables θ_1 and θ_2 .

The expression for the spontaneous magnetization was conjectured by Lin *et al* [28] and proved by Baxter and Choy [26]. As with the other heteropolygona lattices Λ , M can be written (where it is non-zero) as a prefactor times $(1 - (k_{<,\Lambda})^2)^{1/8}$. Let us define (using the subscript $4-8$ to denote $(4 \cdot 8^2)$)

$$k_{<,(4-8)} = \frac{8z^2(1 - 2z + 4z^2 - 2z^3 + z^4)}{(1 - z)^4(1 + z^2)^2} \quad (6.9)$$

and

$$\alpha = \frac{(1 + z^2)}{(1 + z)^{1/2}(1 - z + 3z^2 + z^3)^{1/2}}. \quad (6.10)$$

Then $M_{4-8} = \alpha(1 - (k_{<})^2)^{1/8}$, i.e.

$$M_{4-8} = \frac{(1 - 4z - z^4)^{1/8}(1 + 4z^3 - z^4)^{1/8}(1 + z^2)^{1/2}(1 - 2z + 6z^2 - 2z^3 + z^4)^{1/4}}{(1 - z)(1 + z)^{1/2}(1 - z + 3z^2 + z^3)^{1/2}} \quad (6.11)$$

within the physical FM phase and, by analytic continuation, throughout the complex-temperature extension of the FM phase; M_{4-8} vanishes identically elsewhere. We observe first that under the transformation $z \rightarrow 1/z$, the numerator of this expression goes into itself times a power of z . It follows that the set of formal zeros of this numerator is invariant under the mapping $z \rightarrow 1/z$. In particular, under this mapping, the first and second quartic expressions in the numerator of M_{4-8} are interchanged, up to an overall power of z : $z \rightarrow 1/z \Rightarrow (1 - 4z - z^4) \rightarrow -z^{-4}(1 + 4z^3 - z^4)$. The roots of these two quartics are therefore reciprocals of each other. Under this mapping, the other two factors, $(1 + z^2)$ and $(1 - 2z + 6z^2 - 2z^3 + z^4)$ transform into themselves, up to overall powers of z , and consequently, their zeros also come in reciprocal pairs (since, furthermore they do not have either of the self-reciprocal numbers $z = \pm 1$ as roots). We note the factorizations

$$1 - 4z - z^4 = [1 - \sqrt{2}(\sqrt{2} + 1)z - (\sqrt{2} + 1)z^2][1 - \sqrt{2}(\sqrt{2} - 1)z + (\sqrt{2} - 1)z^2] \quad (6.12)$$

$$1 + 4z^3 - z^4 = [1 + \sqrt{2}z - (\sqrt{2} - 1)z^2][1 - \sqrt{2}z + (\sqrt{2} + 1)z^2] \quad (6.13)$$

$$1 - 2z + 6z^2 - 2z^3 + z^4 = [1 - 2e^{i\pi/3}z + z^2][1 - 2e^{-i\pi/3}z + z^2]. \quad (6.14)$$

Expression (6.12) has zeros at

$$z_{1\pm} = -\frac{1}{2}[\sqrt{2} \pm (-2 + 4\sqrt{2})^{1/2}] \quad (6.15)$$

$$z_{2\pm} = \frac{1}{2}[\sqrt{2} \pm i(2 + 4\sqrt{2})^{1/2}] \quad (6.16)$$

while expression (6.13) has zeros at

$$(z_{1\pm})^{-1} = \frac{1}{2}[2 + \sqrt{2} \pm (10 + 8\sqrt{2})^{1/2}] \quad (6.17)$$

$$(z_{2\mp})^{-1} = \frac{1}{2}[2 - \sqrt{2} \pm (10 - 8\sqrt{2})^{1/2}]. \quad (6.18)$$

Expression (6.14) has zeros at $z_{3\pm}$ and $z_{3\pm}^*$, where

$$z_{3\pm} = e^{i\pi/3} \pm (e^{2i\pi/3} - 1)^{1/2}. \quad (6.19)$$

Note that $z_{3-} = z_{3+}^{-1}$. These roots have the approximate numerical values

$$z_{1+} = 0.249\ 0384 \quad (z_{1+})^{-1} = 4.015\ 4454 \quad (6.20)$$

$$z_{1-} = -1.663\ 252 \quad (z_{1-})^{-1} = -0.601\ 231\ 83 \quad (6.21)$$

$$z_{2\pm} = 0.707\ 1068 \pm 1.383\ 551i \quad (6.22)$$

$$(z_{2\mp})^{-1} = 0.292\ 8932 \pm 0.573\ 0856i \quad (6.23)$$

$$z_{3+} = 0.840\ 6250 + 2.137\ 255i \quad (6.24)$$

$$z_{3-} = (z_{3+})^{-1} = 0.159\ 3750 - 0.405\ 2045i. \quad (6.25)$$

Only a subset of these formal zeros are zeros of the actual magnetization, namely those which can be reached from within the complex-temperature FM phase (they lie on the border of this phase) where (6.11) holds; the other zeros are spurious, since they occur at points which cannot be reached in this manner, where consequently the formula does not apply. The true zeros of M are at $z_c = z_{1+}$, $1/z_{1-}$, z_{3-}^* , and z_{3-} . The first two of these are, respectively, the physical critical point and the point at which the left boundary of the complex-temperature FM phase crosses the real z axis. As one can see from figure 7(a), z_{3-}^* lies where certain areas of zeros of the partition function degenerate to a single point separating the complex-temperature FM and O_2 phases, and similarly for the complex conjugate point z_{3-} separating the FM and O_2^* phases. Indeed, these four points are precisely the full set of points on the border of the complex-temperature FM phase where various areas of zeros degenerate to single points. The exponents with which M_{4-8} vanishes continuously at these zeros are all equal to $\frac{1}{8}$. As one moves upward, away from the origin along the $\text{Im}(z)$ (vertical) axis in figure 7(a), one encounters a boundary followed by a dense set of points where the free energy is non-analytic before one reaches the point $z = i$. This boundary prevents analytic continuation, so that the zero at $z = i$, and similarly, the zero at $z = -i$, in the expression (6.11) are not true zeros of M . Note that the points $\pm i$ lie where the O_1 and PM phases are directly adjacent, and separated by these points. Similarly, all of the remaining zeros in the numerator of the expression (6.11) are not actual zeros of M . Finally, none of the the apparent divergences in M_{4-8} actually occur, since they all lie outside of the FM phase where (6.11) applies.

As with other bipartite lattices, the staggered spontaneous magnetization $M_{st,4-8}$ is given by (3.1) in terms of M_{4-8} in the complex-temperature extension of the AFM phase and vanishes elsewhere. We may thus read off the zeros of $M_{st,4-8}$ immediately; these are precisely the inverses of the four zeros of M , i.e., z_c^{-1} , z_{1-} , $(z_{3-})^{-1} = z_{3+}$, and $(z_{3-}^*)^{-1} = z_{3+}^*$. The first point is the physical critical point separating the PM and AFM phase. The second is the point where the boundary between the AFM and O phases crosses the negative real z axis. The third is where the border between the O_3 and AFM phases narrows to zero thickness, and similarly for the fourth point, separating the O_3^* and AFM phases. The actual zeros of M and M_{st} are listed in table 2.

In table 3 we compare the general properties of the complex-temperature phase diagrams for the Ising model on homopolygonal and heteropolygonal 2D Archimedean lattices, in

terms of the variable z , or equivalently, v . Since we have already indicated in table 2 which lattices have AFM phases, and since all have PM and FM phases, we do not include that information here. The entries in the column marked N_O are the number of O phases. We observe that the Ising model on heteropolygona lattices exhibits more of these O phases than on homopolygona lattices. As we have discussed in our earlier papers [11, 12], the points at which the curves (or line segments, if present) cross are singular points of the algebraic curves, in the technical terminology of algebraic geometry [20]. This usage of the term should, of course, not be confused with the different meaning of ‘singular point’ in statistical mechanics; for example, the point $z_c = (-1 + 2/\sqrt{3})^{1/2}$ of the Ising model on the kagomé lattice is a singular point (actually, the physical critical point separating the PM and FM phases) in the statistical mechanical sense, but is not a singular point of the curve forming the outer boundary of the complex-temperature FM phase, in the algebraic geometry sense (see figure 5(b)). A singular point of the algebraic curve is denoted as a multiple point of index n_b if n_b branches (arcs) of the curve pass through the point. (We use the terms ‘multiple point’ and ‘intersection point’ synonymously here.) In the column marked ‘Mult. pt’, we list information about these multiple points, including the number and the index. The symbol CC means that the multiple points occur in complex conjugate pairs, while ‘real’ means that the multiple points occur on the real axis in the z (equivalently, v) plane. For a normal double point, i.e. a multiple point of index 2, one may assign an angle θ_{cr} as the angle between the tangents of the two branches (arcs) of the curve which pass through the point. All three homopolygona lattices have multiple points on the curves (including line segments) across which the free energy is non-analytic. Each of these multiple points has index 2 and $\theta_{cr} = \pi/2$, i.e. the two branches cross in an orthogonal manner. Our results as shown in figures 5 and 6 show that the multiple points for the $(3 \cdot 6 \cdot 3 \cdot 6)$ and $(3 \cdot 12^2)$ lattices also have index 2 and $\theta_{cr} = \pi/2$. Note that because the transformation (2.3) relating z and v and also the transformation $u = z^2$ are conformal mappings, they preserve angles, so that a given θ_{cr} is the same for a multiple point in the z , v , and u plane. For all of these four lattices, the multiple points occur as complex conjugate pairs as functions of z . A general observation is that the heteropolygona lattices have more multiple points on their curves than the homopolygona lattices. The situation with the $(4 \cdot 8^2)$ lattice is the most complicated, since in this case the loci of points where the free energy is non-analytic form areas instead of curves. As one can see from figure 7, there are a number of multiple points through which more than one of the boundaries of these areas pass. There are 18 such points in all; of these, 14 consist of complex conjugate pairs while the remaining four lie on the real z or v axis. Of the 14 complex conjugate multiple points, 12 have index $n_b = 2$ (with various values of crossing angles θ_{cr}). The four multiple points lying on the real axis (namely, $z_c = z_{1+}$, $1/z_c$, z_{1-} , and $1/z_{1-}$) have index $n_b = 2$ and $\theta_{cr} = 0$. In the terminology of algebraic geometry, they are therefore (simple) tacnodes. We recall that a (simple) tacnode is defined as a multiple point of an algebraic curve through which two branches pass, in an osculating manner, i.e. such that their tangents coincide where the branches touch, so that $n_b = 2$ but the number of distinct tangents at the point is $n_t = 1$ [20]. We have denoted this in tables 2 and 3 by the notation ‘tn’, standing for ‘tacnode’. A generalized tacnode is a multiple point of an algebraic curve for which some of the tangents of the branches passing through the point coincide, so that $n_b > n_t$ (and n_b may be greater than 2). The $(4 \cdot 8^2)$ lattice is the first one which we have studied which exhibits tacnodal points on the loci of points where the free energy is non-analytic. We come next to the multiple points at $\pm i$. These are, again, of a type unprecedented in any of the cases which we have previously studied; they have index 4 and are the first example of a multiple point of index higher than 2. Of the four branches which pass through this point, two cross at an angle of $\pi/2$ with respect to each other, the north-

Table 3. Comparison of some properties of complex-temperature phase diagrams, as functions of z or equivalently v , for the Ising model on homopolygona l and heteropolygona l Archimedean lattices. N_O denotes the number of O phases. In the column marked 'mult. pt', the entry 2:2, cc means that there are two multiple points, each of index 2, and they occur as complex conjugate pairs, etc, for other entries. The notation 'tn' means a tacnodal multiple point. For the $(4 \cdot 8^2)$ lattice we have listed the properties of the various types of multiple points underneath the general number, 18. See the text for further discussions.

Lattice	N_O	Mult. pt	Endpt
sq (4^4)	1	2:2, cc	0
tri (3^6)	1	2:2, cc	2, cc, in FM
hex (6^3)	0	2:2, cc	2, cc, in PM
$(3 \cdot 6 \cdot 3 \cdot 6)$	2	4:2, cc	4, cc, in PM
$(3 \cdot 12^2)$	2	4:2, cc	4, cc, in PM
$(4 \cdot 8^2)$	3	18; see below: 12:2, cc 2:3, cc, tn ($\pm i$) 4:2, real, tn	0

east-south-west and north-west-south-east curves), while two others pass through the points in a north-south direction, hence with a crossing angle of $\pi/4$ with respect to the former two curves and a crossing angle of 0 with respect to each other. This multiple point is therefore a higher-order tacnodal point, with $n_b = 4$ and $n_t = 3$. Finally, in the last column of table 3 we list the number of endpoints of the algebraic curves and in which complex-temperature phase these endpoints lie. For all cases, the endpoints occur in complex conjugate pairs.

For lattices with even q , namely the square, hexagonal, and kagomé lattices, a more compact way to present the complex-temperature phase diagrams is in the u plane. Thus, in the u variable, the entries for these three respective lattices analogous to those listed in table 3 are as follows: $N_O = 0, 0, 1$; multiple points: (1:2, real), (1:2, real), and (2:2, cc); endpoints: 0, (1, real, in FM), and (2, cc, in PM).

7. Conclusions

In this paper, using exact results, we have determined the complex-temperature phase diagrams and singularities of the spontaneous magnetization on three heteropolygona l Archimedean lattices, $(3 \cdot 6 \cdot 3 \cdot 6)$ (kagomé), $(3 \cdot 12^2)$, and $(4 \cdot 8^2)$ (bathroom tile). This study reveals a rich variety of complex-temperature singularities and provides an interesting comparison with the situation for the three homopolygona l lattices. In particular, we have found the first example of a lattice where, even for equal spin-spin exchange couplings, the non-trivial non-analyticities of the free energy lie in areas rather than on curves, in the z (or equivalently, v) plane. We have also given a simple explanation of why this happens.

Acknowledgment

This research was supported in part by the NSF grant PHY-93-09888.

References

- [1] Onsager L 1944 *Phys. Rev.* **65** 117
- [2] Yang C N 1952 *Phys. Rev.* **85** 808

- [3] Domb C 1960 *Adv. Phys.* **9** 149
- [4] Fisher M E 1965 *Lectures in Theoretical Physics* vol C (Boulder, CO: University of Colorado Press) p 1
- [5] Thompson C J, Guttmann A J and Ninham B W 1969 *J. Phys. C: Solid State Phys.* **2** 1889;
Guttmann A J 1969 *J. Phys. C: Solid State Phys.* **2** 1900
- [6] Domb C and Guttmann A J 1970 *J. Phys. C: Solid State Phys.* **3** 1652
- [7] Guttmann A J 1975 *J. Phys. A: Math. Gen.* **8** 1236
- [8] Itzykson C, Pearson R and Zuber J B 1983 *Nucl. Phys. B* **220** 415
- [9] Marchesini G and Shrock R E 1989 *Nucl. Phys. B* **318** 541
- [10] Enting I G, Guttmann A J and Jensen I 1994 *J. Phys. A: Math. Gen.* **27** 6963
- [11] Matveev V and Shrock R 1995 *J. Phys. A: Math. Gen.* **28** 1557
- [12] Matveev V and Shrock R 1995 Complex-temperature singularities in the $d = 2$ Ising model: II triangular lattice; III honeycomb lattice (hep-lat/9411023; hep-lat/9412076) *J. Phys. A: Math. Gen.* at press
- [13] Matveev V and Shrock R 1995 Complex-temperature properties of the 2d Ising model on heteropolygonal lattices hep-lat/9412105 *J. Phys. A: Math. Gen.* **28** at press
- [14] Grünbaum B and Shephard G 1989 *Tilings and Patterns: an Introduction* (New York: Freeman)
- [15] Utiyama T 1951 *Prog. Theor. Phys.* **6** 907
- [16] Syozi I 1972 *Phase Transitions and Critical Phenomena* vol 1 ed C Domb and M S Green (New York: Wiley) p 269
- [17] Laves F 1930 *Z. Kristall.* **73** 202; 1931 *Z. Kristall.* **78** 208
- [18] van Saarloos W and Kurtze D 1984 *J. Phys. A: Math. Gen.* **17** 1301
Stephenson J and Couzens R 1984 *Physica* **129A** 201
Wood D 1985 *J. Phys. A: Math. Gen.* **18** L481
Stephenson J 1986 *Physica* **136A** 147
Stephenson J and van Aalst J 1986 *Physica* **136A** 160
Stephenson J 1988 *Physica* **148A** 88 107
- [19] Kano K and Naya S 1953 *Prog. Theor. Phys.* **10** 158
- [20] Lefschetz S 1953 *Algebraic Geometry* (Princeton, NJ: Princeton University Press)
Hartshorne R 1977 *Algebraic Geometry* (New York: Springer)
- [21] Naya S 1954 *Prog. Theor. Phys.* **11** 53
- [22] Syozi I 1955 *Rev. Kobe Univ. Mercantile Marine* **2** 21
- [23] Huckaby D 1986 *J. Phys. C: Solid State Phys.* **19** 5477
- [24] Lin K Y and Chen J L 1987 *J. Phys. A: Math. Gen.* **20** 5695
- [25] Vaks V G, Larkin A I and Ovchinnikov Yu N 1966 *Sov. Phys.—JETP* **22** 820 (*Zh. Eksp. Teor. Fiz.* **49** 1180)
- [26] Baxter R J and Choy T C 1988 *J. Phys. A: Math. Gen.* **21** 2143
- [27] Wu F Y and Lin K Y 1987 *J. Phys. A: Math. Gen.* **20** 5737
- [28] Lin K Y Kao C H and Chen T L 1987 *Phys. Lett.* **121A** 443
- [29] Syozi I and Naya S 1960 *Prog. Theor. Phys.* **23** 374; *Prog. Theor. Phys.* **24** 829
- [30] Baxter R J 1986 *Proc. R. Soc. A* **404** 1